

OPTIMIZATION OF THE WAVE-MAKING CHARACTERISTICS OF FAST FERRIES

Justus Heimann, Technical University Berlin, Germany

heimann@ism.tu-berlin.de

Stefan Harries, FRIENDSHIP-Systems, Berlin and Technical University Berlin, Germany

harries@FRIENDSHIP-Systems.com

SUMMARY

Fast displacement-type and high-speed ships consume a substantial amount of energy even when sailing in relatively calm water. A considerable resistance component stems from the steady ship wave system. The waves generated also cause adverse effects in the far field as the wash hits a beach or other vessels. It therefore is mandatory to reduce wave-making as much as possible. In order to do so early in the design process a sophisticated shape optimization approach has been developed in which advanced parametric modeling and shape manipulation applying the FRIENDSHIP-Modeler by FRIENDSHIP-Systems, CFD based hydrodynamic analysis utilizing the well-established SHIPFLOW code by Flowtech and detailed performance assessment using the new wave pattern analysis software SWASH by TU Berlin are highly integrated and controlled via the state-of-the-art optimization environment modeFRONTIER by Esteco.

The paper presents all aspects of this approach. Special attention will be given to spectral wave pattern analyses that facilitate the examination of the cause and effect between shape characteristics and wave generation. An elaborated example will be presented for a RoPax ferry typical of fast short-sea shipping featuring a bulbous bow and a tunneled stern. Methods and results will be discussed from both a theoretical and a practical point of view.

1. INTRODUCTION

Can we still squeeze out a few percent? Would we not like to know more about the design space we find ourselves in?

In naval architecture we often face the predicament of coming up with a good hull shape within the tight corset of many constraints from many different fields – safety and comfort, cargo capacity and handling to mention just a few. Once a feasible solution is identified the design team often lacks the resources in time and budget to undertake an extensive search for further improvement. It would therefore be quite nice to let the computer do much more of the busy-work itself and, thus, gain the freedom to focus on decision-making. A promising course adopted to accomplish the task of investigating many designs in a reasonably short time is automated optimization by means of parametric modeling as discussed for instance in [1].

Simply put, automated optimization is the formal process of finding a good (the best) solution from a set of feasible alternatives. It requires a complete mathematical problem formulation in terms of objective functions (what is to be improved), free variables (what shall be consciously changed) and constraints (what restricts the feasibility). Within this paper we will follow this line of thought and focus on hydrodynamic design. We assume the somewhat idealized situation of optimizing an initial hull with the objective of minimizing the energy associated with its wave formation.

Many schemes utilize integral wave resistance values derived from pressure integration as objective function. In this way, however, information is lost on where beneficial and adverse effects originate. A more detailed examination is attainable on the basis of the spectral distribution of wave energy along the components of the steady ship wave system, see e.g. [2] and [3]. An adequate method of wave pattern analysis is therefore discussed which primarily builds on longitudinal wave cuts and treats cuts of finite length with a special truncation correction. In this way the energy loss associated with the transverse and diverging waves can be studied more clearly. Furthermore, the impact of local hull variations on the individual components of wave formation can be traced by investigating the changes in wave spectra with respect to the associated hull variations. A further advantageous effect of the approach is that computed wave patterns and, consequently, the resistance calculations based on them, prove to be less sensitive to flow field discretization than pressure integration.

The example ship chosen for the optimization exercise is that of a fast ferry called FantaRoRo that was devised as an elaborate test case within the European R&D project FANTASTIC, see [4] for an overview on FANTASTIC. The FantaRoRo test case was set up by the consortium to study the potential of the tools developed or improved throughout the project. Several alternative optimization schemes were applied by various partners. The purpose of this paper is to present the details of the approach developed at the Technical University Berlin. For details on the FantaRoRo study see [5].

Figure 1 shows the lines plan of the example ferry. The main particulars of the design are summarized in tab. I. Key constraints for the optimization are given in tab. II. As can be seen from tab. II we allowed ourselves a tangible freedom in shape modification so as to better see merits (and shortcomings).

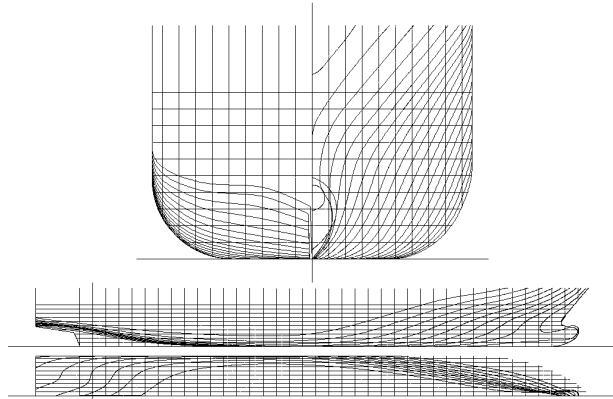


Fig. 1: FantaRoRo parent hull shape

Tab. I: Main particulars of FantaRoRo

L_{PP}	122.74 m	Length between perpendiculars
B	19.2 m	Maximum breadth molded
T	5 m	Design draft
∇	6584 m ³	Displacement volume
C_B	0.549	Block coefficient
x_{CB}	57.8 m	Longitudinal center of buoyancy from AP
A_{WP}	1836 m ²	Waterplane area
V_S	21 kn	Design speed
F_n	0.311	Froude number

Tab. II: Key optimization constraints

No changes aft of the maximum section		
No changes in draft and breadth		
L_{maxAP}	128 m	Maximum length forward of AP
$\Delta \nabla$	$\pm 1\% \nabla$	Maximum change of volume
Δx_{CBaft}	0.6 m	Maximum aftward shift of x_{CB}
Δx_{CBfor}	0.7 m	Maximum forward shift of x_{CB}

2. PARAMETRIC MODELING

In parametric modeling the design problem is formulated partly or even fully in terms of parameters. Parameters are the descriptors of the product to be developed and the product is represented at a much higher level than by point data alone as still done very often.

In the context of optimization a parametric approach has an inherent advantage. While in a non-parametric approach the number of free variables – e.g. point data – that govern the problem rapidly becomes prohibitively high and the fine tuning of the variables to achieve a desirable result often gets very demanding, a parametric approach contents with just a few, but carefully selected form parameters to generate desirable shapes still leaving enough freedom for shape modification.

Consequently, for the optimization presented here a fully-parametric design tool was utilized: The

FRIENDSHIP-Modeler. The tool originates in research performed at the Technical University Berlin, see [6], and a substantially extended and enhanced version for the design of ships and yachts is available from FRIENDSHIP-Systems, see website in reference list.

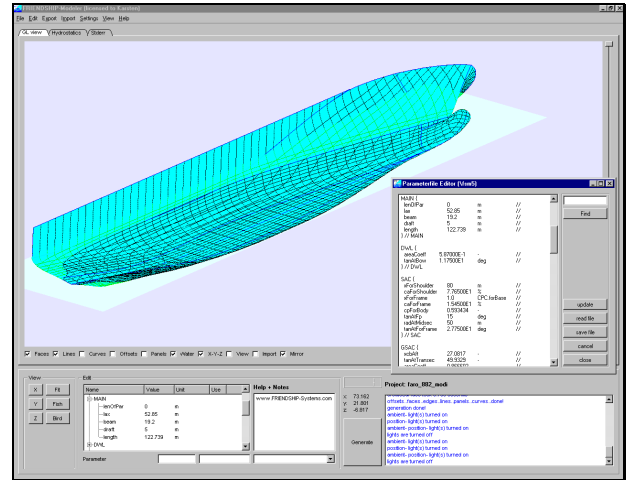


Fig. 2: GUI of FRIENDSHIP-Modeler with excerpt of form parameter file and perspective view of 882*modi

The FRIENDSHIP-Modeler's key feature is a fully-parametric shape description. Each hull – be it a sailing yacht or a ship featuring a bulb – is generated in a three stage process. The entire model is based on B-splines curves and surfaces which are optimized for fairness.

Figure 2 shows the graphical user interface (GUI) of the FRIENDSHIP-Modeler, featuring an improved version of the RoPax ferry (882*modi) in perspective view.

3. PERFORMANCE ASSESMENT

3.1. FLOW ANALYSIS

Within our optimization exercise ship performance is viewed in terms of the wave-making characteristics. More precisely, our aim was to minimize the energy losses associated with the wave formation along the hull.

First of all this calls for a deeper insight into ship wave formation. Thus a hydrodynamic analysis was carried out with the well-known SHIPFLOW code, see website in reference list. SHIPFLOW's Rankine panel module was used to compute the nonlinear free-surface flow. (Complementing computations were undertaken with SHIPFLOW's boundary layer module.) Important quantities that SHIPFLOW provides from nonlinear free-surface flow computations are longitudinal and transverse wave cuts, the hull pressure distribution, dynamic trim and sinkage and the wave resistance from pressure integration over the wetted surface.

3.2. WAVE PATTERN ANALYSIS

Initially, the wave resistance from pressure integration was chosen as the prime objective function for optimiza-

tion, following the methodology laid out in [7]. Extending this, a sophisticated wave cut analysis was utilized for performance assessment. SWASH, a tool developed at the Technical University Berlin, was applied for longitudinal wave cut analyses, see [3]. It yields the wave pattern resistance R_{WP} while – by convention – a pressure integration provides the wave resistance R_w .

SWASH utilizes a longitudinal wave cut method following Sharma, see [8] and [9]. Essential assumptions of the method are ideal flow and the existence of so called ‘free waves’ at sufficient distance from the ship. Though SHIPFLOW computes the fully nonlinear ship wave system, the wave pattern analysis itself is based upon linearized theory assuming only a weak effect of nonlinear contributions.

Formally, the wave pattern resistance can be deduced from conservation of momentum in a control volume which contains the steady ship wave system composed of a superposition of plane progressive waves of all feasible wave directions (θ) and varying wave amplitudes in compliance with the steadiness condition for the phase velocity. In a notation going back to Havelock, the wave pattern resistance is computed from

$$R_{WP} = \frac{\rho V_S^2}{k_0^2} \pi \int_0^{\pi/2} [A_S^2(\theta) + A_C^2(\theta)] \cos^3(\theta) d\theta, \quad (1)$$

where V_S and $k_0 = g/V_S^2$ (infinite water depth), denote the ship speed and the basic wavenumber, respectively. From the wave pattern resistance coefficient

$$C_{WP} = \frac{R_{WP}}{0.5 \rho V_S^2 S_{ref}} = \int_0^{\pi/2} C_{WP}(\theta) d\theta, \quad (2)$$

an extremely useful and descriptive chart, as will be evident later, is obtained by plotting the integrand of (2) as function of wave direction:

$$C_{WP}(\theta) = \frac{\pi}{0.5 S_{ref} k_0^2} [A_S^2(\theta) + A_C^2(\theta)] \cos^3(\theta), \quad (3)$$

with S_{ref} being the reference surface area for normalization (usually the wetted surface at rest). The terms A_S and A_C in (1) and (3) represent the sine and cosine components of the free wave spectra, respectively. $A_{S,C}$, also known as amplitude functions, may be directly derived from Fourier transforms of a longitudinal wave cut. They yield a direct measure of the wave energy distribution along the components of the ship wave system. Hence, the challenge of hydrodynamic optimization based on wave pattern resistance is to reduce the magnitude of the free wave spectra components as much as the constrained problem allows.

In case of flows symmetric to the ship center plane a single infinitely long wave cut parallel to the ship suffices to perform the whole analysis. However, in practical applications due to limited computer resources (CFD) or restrictions due to tank wall reflections (EFD) longitudinal wave cuts need to be truncated at a finite distance downstream of the hull. In order to retain the wave en-

ergy contained within the wave pattern downstream of the truncation point SWASH treats wave cuts of finite length by a special truncation correction. At a sufficiently large distance aft of the stern the wave cut is usually dominated by transverse waves following the ship. This gives rise to utilizing an analytic truncation function composed of harmonic waves decaying to infinity. Finally, to fit the truncation function to the wave cut unknown coefficients are introduced which in turn are determined by a regression analysis of the tail end of the wave cut signal up to the truncation point.

Practical application of longitudinal wave cut analysis mainly depends on the lateral position of the cutting plane, the utilizable length of the wave signal until truncation and the ship’s speed. In order to avoid serious analysis errors and to ensure validity of the method the cut is to stay outside a region close to the hull where local flow effects are predominant. On the other hand the lateral distance needs to be small enough to capture the wave signal as much as possible. According to our experience satisfactory results are obtained for medium speed and fast monohulls at lateral cut positions in the range $0.2 \leq y/L_{pp} \leq 0.3$ (provided the cut extends far enough downstream to allow for a truncation correction). This is in agreement with related studies, e.g. [10].

In the optimization process we systematically applied the wave pattern analysis to examine and to account for the energy loss associated with the transverse and the diverging waves. In this way, information could be gathered on where beneficial and adverse effects originate, allowing us to trace the impact of hull variations on the components of wave formation, particularly the transverse and diverging wave regimes, and vice versa.

An advantageous side-effect of the approach is that computed wave patterns and, consequently, the resistance calculations based on them, prove to be less sensitive to flow field discretization than hull pressure integration, as will be briefly addressed in section 5.

4. HYDRODYNAMIC OPTIMIZATION

Figure 3 depicts the typical process flow of formal hydrodynamic optimization. A very tight integration of four modules is essential for the optimization’s success:

- Shape generation,
- Flow analysis,
- Performance assessment and
- Optimization strategies.

Throughout this study the shape generation was done via the FRIENDSHIP-Modeler. The hydrodynamic analysis was carried out with the SHIPFLOW code. The prime objective function of the optimization was the wave resistance from pressure integration and the wave pattern resistance as derived from a longitudinal wave cut analysis utilizing SWASH. For integration of the various tools and as a GUI-based workbench providing many

different optimization strategies the multi-objective design environment modeFRONTIER was utilized, see website in reference list. A shell script, controlled by modeFRONTIER, was developed at the operating system level to distribute parallel computing tasks among our heterogeneous and distributed hardware resources.

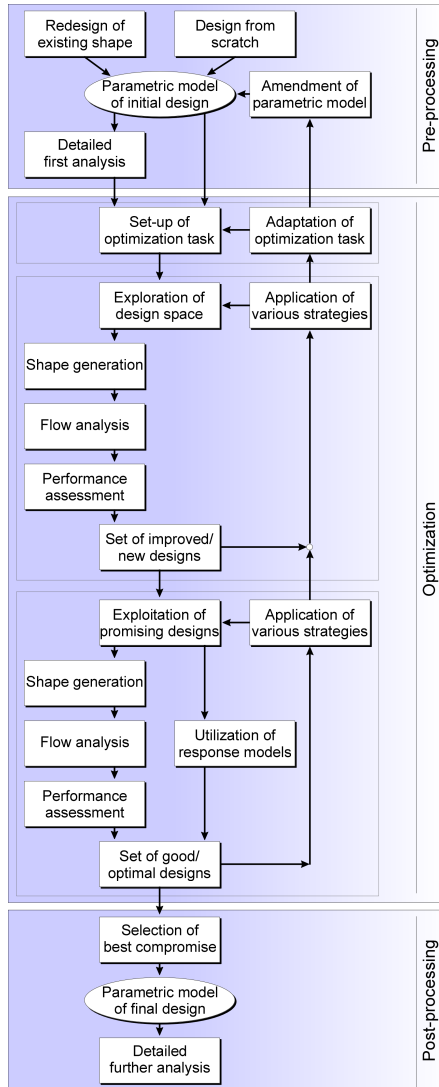


Fig. 3: Process flow in hydrodynamic design

From fig. 3 it can be nicely seen that hydrodynamic optimization is an iterative and interactive design process that should not be confused with a black box that yields the best ship for simple questions asked. Even though many design variants might be automatically assessed at each time an optimization run is started, the entire design procedure requires the users to evaluate and reconsider their problem set-up as the investigation progresses. For further details see [11].

5. TOWARDS OPTIMAL HULL LINES – ELABORATE EXAMPLE

5.1. OPTIMIZATION PROCESS

The optimization set-up as realized with modeFRONTIER

is shown in fig. 4. A set of 15 form parameters was used for modifying the hull shape. The free variables mainly correspond to two basic curves – the design waterline DWL and the sectional area curve SAC (for the entrance) – and the bulbous bow BBOW. In tab. III the parameters of the parent hull and an improved shape (882*modi) are listed along with the (final) bounds on the free variables. Only the forebody was allowed to change, the afterbody was required to stay untouched.

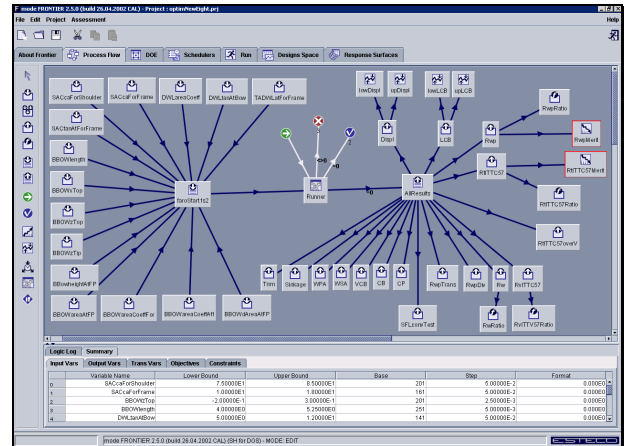


Fig. 4: Optimization set-up in modeFrontier

Tab. III: Form parameters in example optimization

	Free variable / form parameter	Lower bound	Upper bound	Parent hull	882* modi
Entrance parameters	SACcaForShoulder	75 %	85 %	77.91 %	77.65 %
	SACcaForFrame	10 %	18 %	13.20 %	15.45 %
	SACTanAtForFrame	20	60	35	27.75
	DWLtanAtBow	5	12	9.5	11.75
	DWLareaCoeff	0.57	0.65	0.625	0.587
	TADWLatForFrame	60	100	63.128	60.25
Bulbous bow parameters	BBOWareaCoeffFor	0.825	0.925	0.85	0.925
	BBOWareaCoeffAft	0.35	0.45	0.4	0.4
	BBOWareaAtFP	7	10	8.57	10
	BBOWdAreaAtFP	30	50	35	40
	BBOWlength	4	5.25	4.24	5.25
	BBOWheightAtFP	87.5 %	95 %	90 %	87.5 %
	BBOWzTop	-0.2	0.3	-0.08	0.3
	BBOWxTop	60 %	75 %	68 %	73.3 %
BBOWzTip	-1.5	-0.5	-1.15	-0.685	

Inequality constraints were imposed on displacement and longitudinal center of buoyancy, see tab. II. (Actually, the displacement of the bare hull was implicitly kept constant within the FRIENDSHIP-Modeler during the optimization. Slight changes in the overall displacement occurred due to variations in the bulb volume.) Several important quantities like trim and sinkage, waterplane area, wetted surface area etc. were monitored.

As already stated above, the wave pattern resistance R_{WP} and the wave resistance from pressure integration R_W were employed as the major objective functions. For the sake of completeness and in view of the stipulations for the FANTASTIC optimization exercise the total resistance R_T was also taken into consideration, basically fea-

turing the changes in R_W and wetted surface ¹.

For the optimization runs a medium size panelization with 1185 panels covering one half of the hull and 5125 panels for the free surface per symmetric half was employed. The free surface panelization was extended $x/L_{pp} = 2.4$ downstream of the stern in order to allow for an accurate wave cut analysis with truncation correction. The nonlinear flow analysis was restarted from previously converged nonlinear solutions so as to reduce computational effort. Trim and sinkage were free.

Throughout the process several optimization runs were executed. Instead of discussing them all only the last and finest run shall be explained in detail: From the data basis built up in previous optimizations a MOGA (multi-objective genetic algorithm), see [12], was started with 80 carefully selected candidates for the initial population. The wave pattern resistance and the total resistance were utilized as the two competing objectives. A total of 30 generations was generated and traced. Finally, in order to further benefit from the results achieved already a SIMPLEX search according to Nelder and Mead [13] was activated from the very best designs. For the SIMPLEX just one objective was accounted for, namely the sum of R_{WP} and R_W . The SIMPLEX was finally terminated at a stage where improvements became marginal.

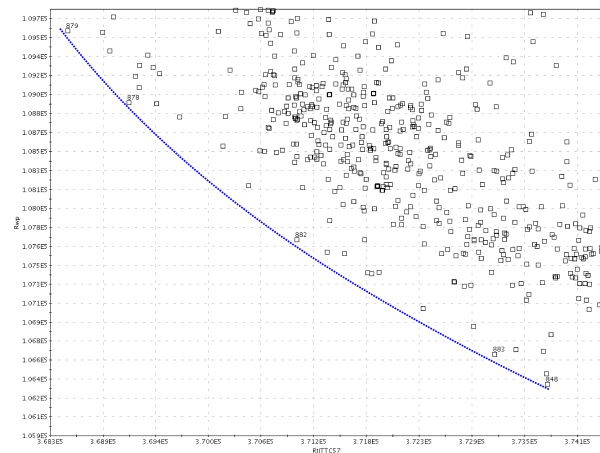


Fig. 5: Scatter diagram, R_{WP} over R_T

Figure 5 depicts the final scatter diagram of R_{WP} vs. R_T . The designs are marked by square boxes while a Pareto front – the set of all solutions for which a single objective cannot be further improved without deteriorating any other objective – is drawn as a dotted curve. Those designs that are closest to the Pareto front display low wave pattern resistance along with low total resistance. Apparently, it is impossible to decrease R_{WP} below certain limits without impairing R_T .

¹ Following Froude’s hypothesis, the viscous component of the total resistance was simply added to the wave resistance component. The frictional resistance was computed from the ITTC 57 friction line, a reasonable form factor was estimated and assumed constant since no changes were permitted in the afterbody.

As part of the final Pareto front in fig. 5 we identified the design #882 as an optimal trade-off promising both a significant reduction of wave generation and a considerable improvement in pressure distribution. For further analyses a slightly modified version of #882 – called 882*modi – was launched. It features pronounced (S-shaped) buttocks resulting from a narrow design waterline and a hook-shaped protruding bulbous bow, see fig. 6. It therefore resembles an interesting deviation from conventional hull shapes. In tab. III and IV data for the parent and the significantly improved hull 882*modi, also referred to as the optimal hull, are given.

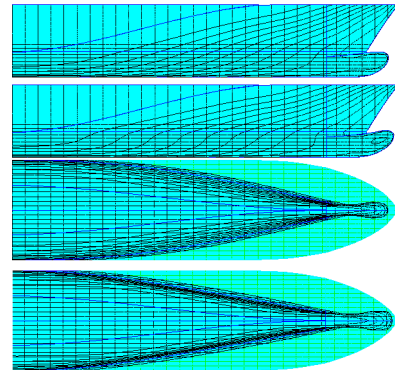


Fig. 6: Forebody side and top view, respectively, of the parent (top) and the optimal hull 882*modi (bottom)

Within the scope of the FANSTASTIC project model tests were conducted by SSPA, Göteborg, which confirmed the optimization outcome by means of a comparative study, see [5] for an elaboration.

5.2. FURTHER ANALYSIS

Based on the optimization outcome, we posed the following questions: Is it possible to identify an accumulation of effects of various optimized hull regions on wave formation, e.g. the whole bulb or the entrance (of the 882*modi)? Or would a simple summation of the single effects of various local hull variations do reveal their joint impact on wave formation? And, if this holds true, can we use this insight to improve shape optimization? Prior to its verification, the answer is Yes – Yes, at least for our RoPax ferry example!

It should be elaborated on this by presenting a small numerical experiment. We simply took the parent hull and replaced its initial bulb by the optimal bulb of the 882*modi, leaving the remaining hull untouched. At the modeling stage this was simply achieved by adjusting the parameter set of the parent hull by the optimal bulbous bow parameters of the 882*modi, leaving all other parameters as before. The resulting hybrid shape, i.e., the parent hull with optimal bulb, was called Optimal bulb. The form parameters in question are indicated by ‘bulbous bow parameters’ in tab. III. In order to complete our experiment we created an opposite hybrid, i.e., this time solely the entrance of the parent hull was replaced by the optimal entrance (from FP to midship) of

the 882*modi, again leaving the remaining hull, including the bulb, untouched. The necessary form parameter changes are indicated by ‘entrance parameters’ in tab. III. This second hybrid hull was called Optimal entrance, i.e., the parent hull with optimal entrance.

Tab. IV: Comparison of resistance gains ($F_n = 0.311$)

Resistance components	Parent hull	882*modi	Optimal bulb	Optimal entrance
$R_{T_{ITTC57}}$ [kN]	403.6	378.5	388.4	394.6
Gain [%]	–	6.2	3.8	2.2
R_W [kN]	165.7	138.9	149.2	156.3
Gain [%]	–	16.2	10.0	5.7
R_{WP} [kN]	136.0	115.8	127.9	123.5
Gain [%]	–	14.9	6.0	9.2
R_{WP} transverse [kN]	98.8	81.5	93.3	86.5
Gain [%]	–	17.6	5.6	12.4
R_{WP} diverging [kN]	37.2	34.3	34.6	36.9
Gain [%]	–	7.8	6.9	0.7
S [m ²]	2479	2497	2493	2483

Tab. V: Comparison of percentage gains in R_W and R_{WP} in relation to the maximum gains of 882*modi²

Relative percentage resistance gains	Optimal bulb	Optimal entrance	Σ
relative gain in R_W [%]	62	35	97
relative gain in R_{WP} [%]	40	62	102
relative gain in R_{WP} transverse [%]	32	71	103
relative gain in R_{WP} diverging [%]	88	9	97

For a thorough comparison further flow analyses were conducted: Four hull forms, the parent hull, the optimal hull 882*modi and the two hybrid hulls Optimal bulb and Optimal entrance were evaluated on an 1.5 times denser panel mesh (ten thousand panels in total) compared to that used for the optimization runs. To gather much of the shorter wavelength effects, parallel to the hull more than 40 free surface panels per fundamental wavelength ($\lambda_0/L_{pp} = 0.61$) were placed longitudinally.

The numerical results are presented in tab. IV and V. Figure 7 shows the hull pressure distributions and in fig. 8 nonlinear wave patterns are compared. Finally, fig. 9 and 10 depict charts of the wave cuts and the wave pattern resistance coefficients from wave cut analyses, respectively.

As anticipated a priori the optimal hull 882*modi performs best in all categories. Both the wave generation and thus R_{WP} and the wave resistance R_W due to an improved pressure distribution were significantly reduced. Table IV and fig. 10 reveal that the major portion (85%) of wave pattern resistance improvement is attained by a reduction of the transverse wave components comprising wave directions up to 35°. Whereas, the reduction of the diverging waves as associated with the wave direc-

² Small deviations from a total of 100% indicate that the superposition of the single effects of both, the optimal bulb and the optimal entrance, respectively, do not ideally add up to fully match the 882*modi.

tions above 35° contributes only by 15%. This might be evident, since here, more than 70% of the total wave pattern resistance are dissipated by the transverse waves.

From this numerical experiment some remarkable conclusions can be drawn:

- Accumulated effects of optimized hull regions on wave formation are apparent, since the optimal bulb shows a reduction of diverging waves while on the other hand the optimal entrance effected the transverse waves most favorably (tab. IV and V and fig. 10).
- The principle of superposition is applicable. For instance, the simple summation of the individual effects of both, the optimal bulb and the optimal entrance, respectively, proved to very closely match the optimal hull 882*modi (fig. 9 and 10) This applies to the wave formation but also to the hull pressure distribution (fig. 7).
- Even the impact of local hull variations on wave formation can be effectively traced. Tests with single parameter variations (e.g. the bulb length alone) in the same manner revealed the validity of the principle of superposition. (No further results are presented here for lack of space.)

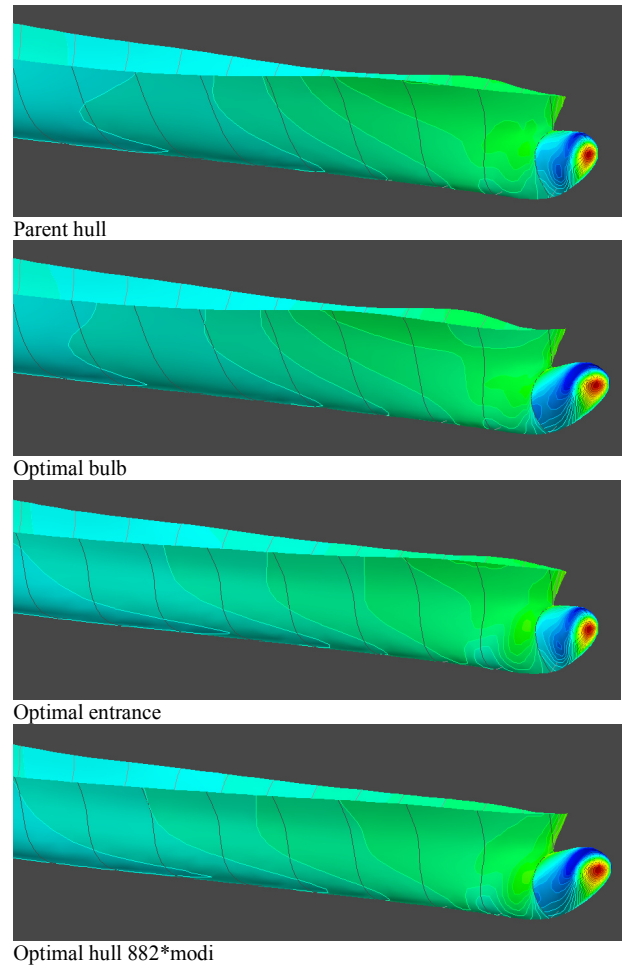


Fig. 7: Comparison of hull pressure distributions from potential flow analyses including the free-surface

Furthermore, the first two rows of tab. V point out that for the optimal bulb and entrance, respectively, the gains

in wave resistance R_W from pressure integration and those in wave pattern resistance R_{WP} from wave analysis are in opposite relationship to each other. This surprising result is in alignment with experiences made during the optimization runs were, sometimes, R_W and R_{WP} pointed into opposite directions. One might argue that this phenomenon cannot be purely explained by the observation that computed wave patterns and, consequently, the resistance calculations based on them, prove to be less sensitive to flow field discretization than hull pressure integration. The reason for this, somewhat disturbing, result has to be further investigated.

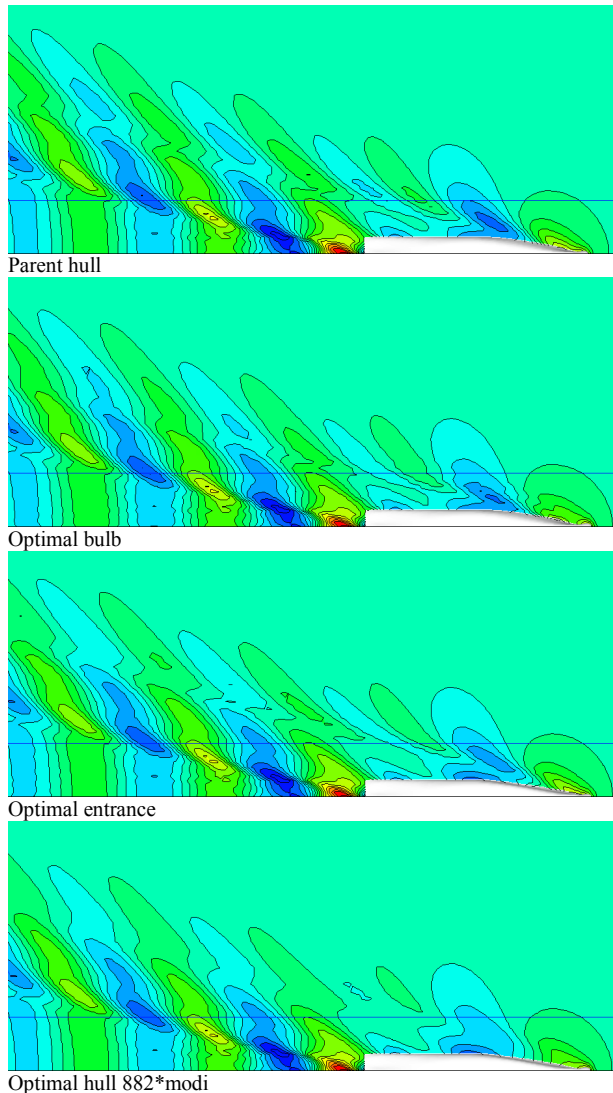


Fig. 8: Comparison of wave contours from nonlinear free-surface potential flow analyses ($F_n = 0.311$)

Finally, in view of the results we were tempted to test whether the optimization only with a form parameter subset would move into the same direction as using the whole parameter set at once. A sequential optimization each with a small form parameter subset promises to be faster and much easier than working on the whole set at once. Consequently, as an example, we selected only the entrance parameters as free variables. A further SIMPLEX optimization was executed from the same

starting point as already outlined in section 5.1, again with the sum of R_{WP} and R_W as objective function. The result achieved is promising, insofar as the optimal entrance parameters have moved in the same direction, but amplified in magnitude, compared to the outcome when optimizing all form parameters at once. Further studies are necessary to determine the applicability of successive optimization of hull regions.

6. CONCLUSION

A comprehensive optimization of a fast ferry was presented on the basis of a synthesis model which comprised advanced parametric modeling, state-of-the-art flow analysis and detailed performance assessment. The optimization process features a multi-phase, multi-step, interactive and iterative character whose roots lie in the complexity of hydrodynamic design. The combination of suitable deterministic and stochastic search strategies along with the selection of the free variables and the determination of their bounds is an important issue and needs adjustment during the optimization. The process relies on a complete IT integration as the prerequisite for automated optimization. The automated optimization itself enables the designer to investigate many variants without the overhead of tedious and non-creative work. In a multi-objective problem the best result depends on the designer's preferences.

Performance assessment based on wave pattern analysis has shown to be a valuable instrument in hydrodynamic optimization complementary to wave resistance prediction from pressure integration. Accumulated effects of hull regions or even the impact of local hull variations on wave formation were effectively traced by means of wave pattern analysis and thus utilized for optimization. Furthermore, the principle of superposition can be further employed, thus, allowing a summation of the single effects of various local hull variations in order to reveal their joint impact on wave formation. This gives rise to the successive optimization of confined hull regions.

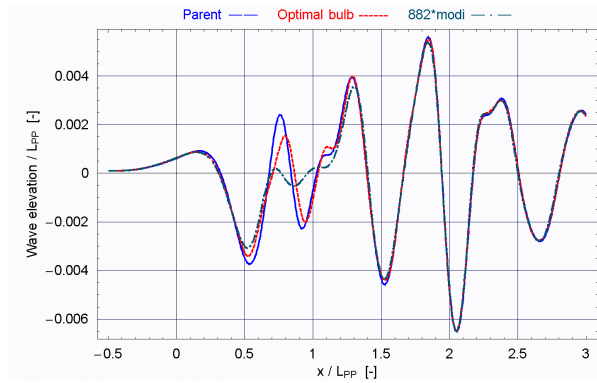
Based on the encouraging results of the presented optimization study research is underway to further improve the shape optimization process even closer focusing on the valuable instrument of wave pattern analysis.

ACKNOWLEDGEMENT

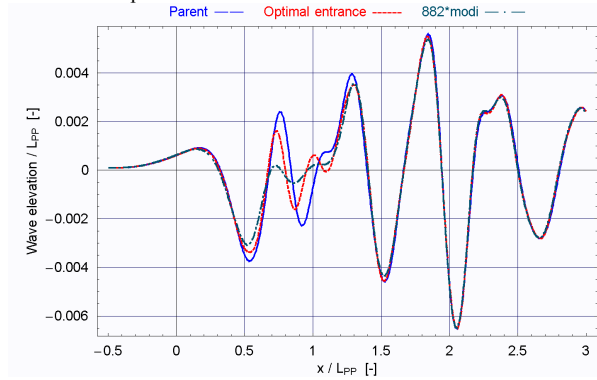
Parts of the research reported in this paper were performed within the European R&D project FANTASTIC – Functional Design and Optimisation of Ship Hull Forms (GRD1-1999-10666 under the 5. FP).

REFERENCES

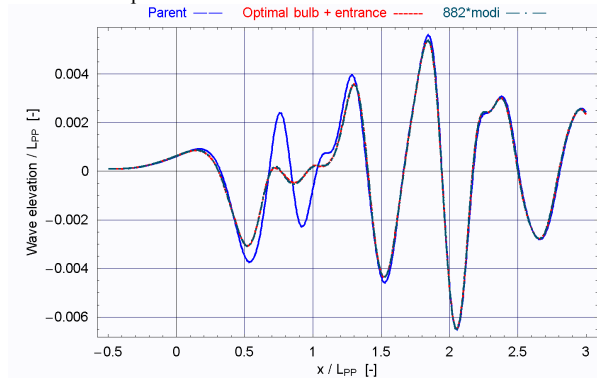
1. BIRK, L.; HARRIES, S., *Automated Optimization – A Complementing Technique for the Hydrodynamic Design of Ships and Off-shore Structures*, 1st Int. Conf. on Computer Applications and Information Technology in the Maritime Industries COMPIT'00, Potsdam, 2000



Effect of the optimal bulb on wave elevation



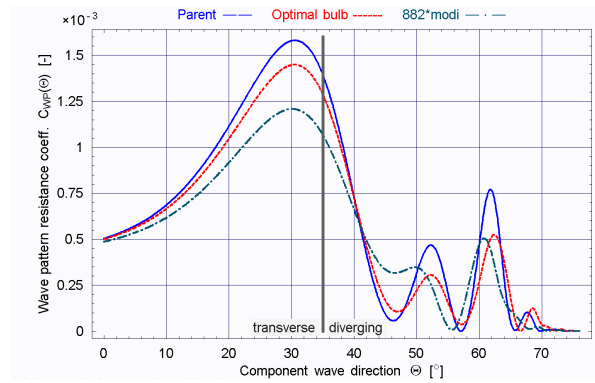
Effect of the optimal entrance on wave elevation



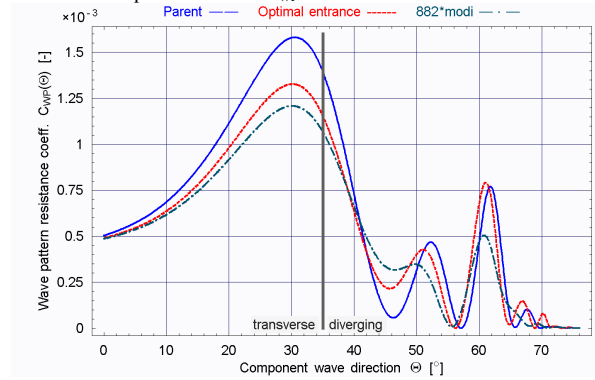
Wave cut of the parent hull superimposed by the wave changes due to both the optimal bulb and the optimal entrance, respectively

Fig. 9: Comparison of longitudinal wave cuts at $y/L_{PP} = 0.25$ ($F_n = 0.311$) from nonlinear free-surface potential flow analyses (FP: $x/L_{PP} = 0$, AP: $x/L_{PP} = 1$)

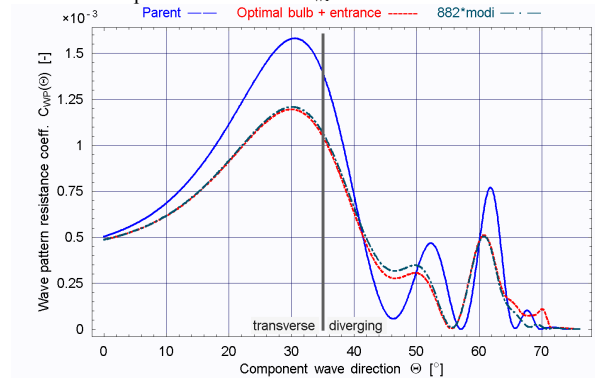
2. NOWACKI, H.; HARRIES, S.; SCHULZE, D.; STINZING, H.-D., *Verification of Wave Cut Design Methodology*, Brite EuRam III Project CALYPSO, Deliverable Report 1.8, Berlin, 1999
3. HEIMANN, J., *Application of Wave Pattern Analysis in a CFD Based Hull Design Process*, 3rd Int. Numerical Towing Tank Symp. NuTTS'00, Tjörn, Sweden, 2000
4. MAISONNEUVE, J.-J.; HARRIES, S.; MARZI, J.; RAVEN, H.C.; VIVIANI, U.; PIIPPO, H., *Towards Optimal Design of Ship Hull Shapes*, 8th Int. Marine Design Conf. IMDC'03, Athens, 2003
5. VALDENAZZI, F.; HARRIES, S.; JANSON, C.-E.; LEER-ANDERSEN, M.; MAISONNEUVE, J.-J.; MARZI, J.; RAVEN, H., *The FANTASTIC RoRo: CFD Optimisation of the Forebody and its Experimental Verification*, Int. Conf. on Ship and Shipping Research NAV'03, Palermo, June 2003
6. HARRIES, S., *Parametric Design and Hydrodynamic Optimization of Ship Hull Forms*, Dissertation, Technical University Berlin, Mensch & Buch Verlag, 1998
7. HARRIES, S.; ABT, C., *Formal Hydrodynamic Optimization of a Fast Monohull on the Basis of Parametric Hull Design*, 5th Int. Conf. on Fast Sea Transportation FAST'99, Seattle, August 1999



Effect of the optimal bulb on C_{WP}



Effect of the optimal entrance on C_{WP}



C_{WP} of the parent hull superimposed by the changes in C_{WP} due to both the optimal bulb and optimal entrance, respectively

Fig. 10: Comparison of wave pattern resistance coefficients C_{WP} as functions of wave direction Θ

8. SHARMA, S.D., *An Attempted Application of Wave Analysis Techniques to Achieve Bow-Wave Reduction*, 6th Symp. on Naval Hydrodynamics, ONR/ACR-136, Washington D.C., 1966
 9. EGGERS, K.W.H.; SHARMA, S.D.; WARD, L.W., *An Assessment of some Experimental Methods for Determining the Wave-Making Characteristics of a Ship Form*, Trans. SNAME, Vol.75, 1967
 10. LALLI, F.; FELICE, F.Di.; ESPOSITO, P.; MORICONI, A.; PISCOPIA, R., *Longitudinal Cut Method Revisited: A Survey on Main Error Sources*, JSR, Vol. 44, No. 2, pp. 120-139, June 2000
 11. ABT, C.; HARRIES, S.; HEIMANN, J.; WINTER, H., *From Re-design to Optimal Hull Lines by Means of Parametric Modelling*, COMPIT'03, Hamburg, May 2003
 12. SPICER, D.; COOK, J.; POLONI, C.; SEN, P., *EP 20082 FRONTIER: Industrial Multiobjective Design Optimisation*, ECCOMAS'98, Published by John Wiley & Sons, Ltd., 1998
 13. PRESS, W.H.; TEUKOLSKY, S.A.; VETTERLING, W.T.; FLANNERY, B.P., *Numerical Recipes in C – The Art of Scientific Computing*, 2nd edition, Cambridge University Press, 1994
- <http://www.esteco.it/>
<http://www.flowtech.se/>
<http://www.friendship-systems.com/>
<http://www.napa.fi/>